engineering proceedings

MDPI

Proceeding Paper

Estimation of the Size of a Growing Crack Through Strain Sensing Under Uncertainty †

Anastasia Valma, Nicholas Silionis and Konstantinos Anyfantis *

Ship–Hull Structural Health Monitoring (SH–SHM) Group, School of Naval Architecture and Marine Engineering, National Technical University of Athens, 15780 Athens, Greece; www.alexpapa@gmail.com (A.V.); nsil@naval.ntua.gr (N.S.)

* Correspondence: kanyf@naval.ntua.gr

† Presented at the 8th International Conference of Engineering Against Failure (ICEAF VIII), Kalamata, Greece, 22–25 June 2025.

Abstract

Fatigue cracks in highly stressed regions of marine structures, caused primarily due to wave loading, are critical life-limiting factors that can lead to structural failure. Structural Health Monitoring (SHM) systems offer the ability to remotely monitor damage progression during its initial phases, enabling failure prevention. One diagnostic approach utilizes the strain redistribution in the vicinity of the crack tip, captured by sensor readings, to inversely calculate the corresponding crack length. This work addresses the challenge of accurately calculating the crack length under variable sources of uncertainty by employing the statistical framework of Maximum Likelihood Estimation (MLE). The method is demonstrated on a simplified test geometry using simulated strain data, registered at locations where structural response sensors may be placed. This approach enables the integration of multiple strain features at modest computational cost, facilitating the assessment of different sensor placement strategies under realistic noise conditions.

Keywords: finite element model; maximum likelihood estimation; crack length; strain measurements

check for updates

Academic Editors: Spiros Pantelakis and Spyros Diplas

Published: 9 December 2025

Citation: Valma, A.; Silionis, N.; Anyfantis, K. Estimation of the Size of a Growing Crack Through Strain Sensing Under Uncertainty. *Eng. Proc.* **2025**, *119*, 3. https://doi.org/10.3390/engproc2025119003

Copyright: © 2025 by the authors. Licensee MDPI, Basel, Switzerland. This article is an open access article distributed under the terms and conditions of the Creative Commons Attribution (CC BY) license (https://creativecommons.org/licenses/by/4.0/).

1. Introduction

In marine structures, particularly ship hulls, fatigue cracks are among the primary life-limiting factors. These cracks originate from microstructural deformations in the material which gradually propagate under cyclic loading, in the case of ship hulls, mainly wave loading, leading to potentially catastrophic failure [1]. Detecting, quantifying and assessing fatigue damage are essential to ensure structural integrity and operational safety.

To achieve this in an accurate and efficient manner, indirect sensing methods have been introduced, employing various types of sensors to obtain real-time insights into crack propagation. This work focuses specifically on structural health monitoring (SHM) through strain sensing. In recent years, various approaches and strain sensor technologies have been proposed to implement strain-based crack monitoring. For example, Han et al. [2] demonstrated the use of novel fibre-optic sensors in conjunction with Brillouin-based analyzers for efficient crack detection and crack width measurement. In another study, Argiris et al. [3] focused on optimizing the positioning of strain sensors, using Bayesian inference, to enhance crack detection performance in plate-like structures.

Additionally, Tatsis et al. [4] developed a hierarchical Bayesian filtering method for online crack detection based only on vibration measurements. Their approach employs

a particle filter at an upper level to estimate crack properties and a set of augmented Kalman filters at a lower level to estimate the system state and unknown input. A different approach using output-only vibrations measurements was proposed by Papadimitriou et al. [5], who estimated fatigue damage accumulation in metallic structures while using Kalman filters and a dynamic model of the structure to predict stress–strain response at locations lacking measurements. Finally, Yu et al. [6] employed piezoelectric wafer active sensors (PWAs), which serve as both actuators and sensors, to enable early-stage crack detection and facilitate both localization and quantification of cracks.

Based on the understanding that a growing crack causes strain redistribution in the vicinity of the crack tip [7], this work utilizes strain measurements within a diagnostic framework. The core challenge addressed here is finding a way to process the strain readings in order to estimate the corresponding crack size under the presence of measurement noise. To this end, a finite element (FE) model of a compact tension CT specimen was developed to simulate strain measurements from a range of potential sensor placement locations as the crack propagates. To overcome the inherent ill-conditioning of this inverse problem in the presence of noisy signals, a probabilistic approach based on Maximum Likelihood estimation (MLE) was employed. Ultimately, the method aims to identify optimal sensor locations for accurate crack length prediction using noisy measurements.

2. Finite Element (FE) Model

To assess the effectiveness of selected strain gauge locations for predicting crack length under uncertainty, it was necessary to generate realistic strain measurements for various crack length inputs. To this end, a Finite Element (FE) model was employed, corresponding to a 2D compact tension CT specimen geometry, constructed using ANSYS 24.2 (Figure 1). A 2D instead of a 3D model was selected, since it is simpler, sufficient for the intended analysis and more computationally efficient.

The model employs a mesh of 8-node plate elements with a characteristic element size of L_e = 1 mm. These are higher-order 2D elements with quadratic displacement behaviour, suitable for modelling both plane stress and plane strain conditions, chosen to accurately capture the strain redistribution caused by crack propagation. The material used in the model is AH36 steel, whose mechanical properties are presented in Table 1, based on values reported in [8,9].

Table 1. Mechanical properties of AH36 steel.

Property	Value	Unit
Young Modulus (E)	200	GPa
Yield Strength (σ_Y)	355	MPa
Ultimate Strength (σ_U)	490	MPa
Fracture Toughness (K_{IC})	180	MPa $m^{1/2}$
Poisson Ratio (v)	0.3	-

A static tensile force equal to 10 kN is applied to the Finite Element (FE) model by connecting the nodes at the loading holes to master nodes at the hole centroids with rigid link elements and applying the tensile force to the master nodes. The boundary conditions were chosen to simulate the constraints imposed by mounting the test specimen on a hydraulic testing machine. Accordingly, nodal displacement along the back face of the specimen was constrained along the y and z directions, while on the loading hole faces, displacement was constrained along the x direction.

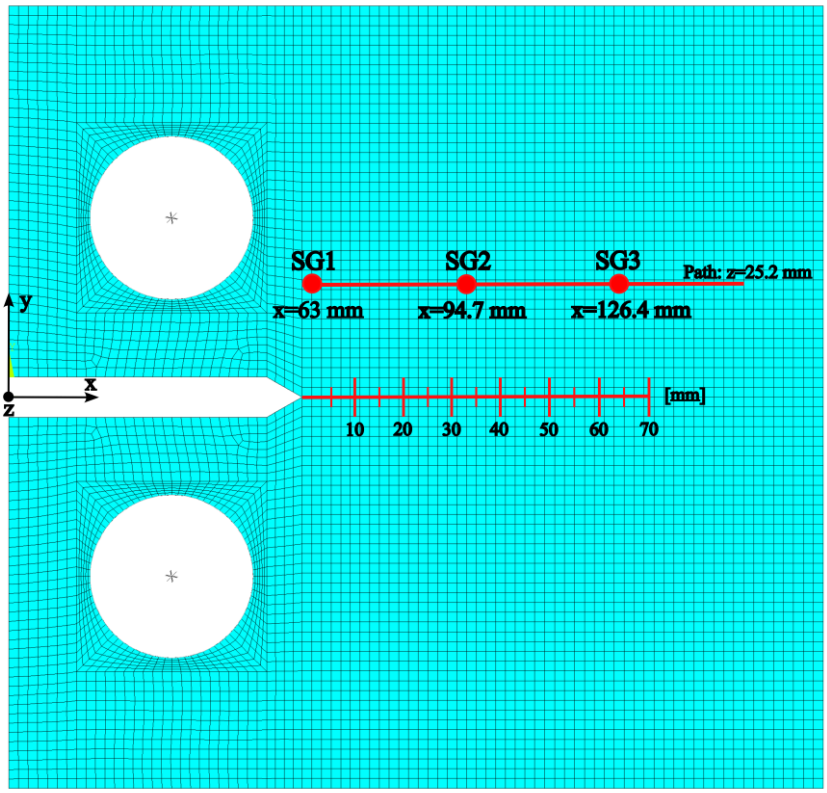


Figure 1. Finite Element (FE) model of the Compact Tension specimen (CT), illustrating the positions of the simulated strain gauges (SG1, SG2 and SG3). The red scale, starting from the notch tip, defines the predicted crack propagation path along the x direction.

Furthermore, each simulated strain gauge is configured as a two-channel rosette, with individual gauges oriented along the x and y directions, parallel to the principal dimensions of the finite element (FE) model, as shown in Figure 1. The width of the model (W = 175 mm) is parallel to the x-axis, and its length (L = 168 mm) aligns with the z-axis. In this study, three strain gauges (SG1, SG2 and SG3) have been employed, positioned at x = 63 mm, x = 94.7 mm and x = 126.4 mm, respectively, along a defined path at y = 25.2 mm.

3. Maximum Likelihood Estimation for FE-Model Accuracy Evaluation

This section introduces Maximum Likelihood Estimation (MLE), a commonly employed statistical method that provides estimates of certain parameters of the data-generating process, under which the observed data are most probable [10]. The MLE approach enables the identification of the crack length that maximizes the likelihood of observing a minimal discrepancy between the finite element (FE) model-predicted strains as a function of crack length and the measured—or, in this case, synthetically simulated—strain data.

3.1. Incorporating Uncertainty Through Gaussian Error Modelling

The foundation of this method is based on a deterministic framework, initially aiming to minimize the Mean Squared Error (MSE) between the measured strain observations ε_i^* and the corresponding finite element model predictions $\hat{\varepsilon}_i$. The difference between these two quantities, representing the error or deviation, is denoted as:

$$e_i = \varepsilon_i^* - \hat{\varepsilon}_i. \quad (1)$$

However, since the analysis is conducted under conditions of uncertainty, each deviation e_i must be assigned a statistical structure. Therefore, each e_i is modelled as a random variable E_i, assumed to follow a normal distribution with zero mean μ and variance σ^2:

$$E_i \sim N(e_i; \mu = 0; \sigma^2 = \sigma_e^2), \tag{2}$$

where

$$E_i = \varepsilon_i^* - f_i(\alpha), \tag{3}$$

where $f_i(\alpha)$ denotes the finite model predicted strain for a combination of sensors i, corresponding to crack length α, which is assumed to follow a normal distribution with mean $f_i(\alpha)$ and variance σ^2, and ε_i* is treated as a constant.

This probabilistic assumption, where the deviation is modelled as a Gaussian random variable, enables the transition from a deterministic error minimization problem to one based on likelihood maximization. Under the assumption of normally distributed errors with constant variance, Maximum Likelihood Estimation (MLE) is mathematically equivalent to minimizing the Mean Squared Error (MSE) [11].

3.2. Maximum Likelihood Estimation Procedure

Accordingly, for the minimization of the deviation random variable E_i, Maximum Likelihood Estimation (MLE) is applied under the assumption that each strain measurement is conditionally independent given the crack length, to enable the joint probability of the observations to be expressed as a product of their individual probabilities [12].

To simulate realistic measurement conditions for comparison with the FE model predictions, synthetic strain observations ε_i* are generated for each target crack length by adding zero-mean Gaussian noise to the corresponding FE strain outputs. In this work, a set of thirty noisy strain observations per strain gauge was produced for each target crack length. These noisy observations are used as a reference dataset against which the comparison is performed.

After acquiring the synthetic strain observations for a target crack length, they are compared against strain predictions obtained from the finite element (FE) model at selected sensor locations, over a finely discretized range of crack lengths using the likelihood function to determine the crack length at which their deviation is most likely to be near zero.

The likelihood function of observing a strain value ε_i* close to the FE model prediction as a function of α ($f_i(\alpha)$), given that the deviation E_i is modelled as a normally distributed continuous random variable with zero mean and variance σ^2, is given by the normal probability density function as follows [12]:

$$L(E_i|a) = P(E_i|a) = f\ (E_i|a) = \frac{1}{\sqrt{2 \cdot \pi \cdot \sigma^2}} \exp\left(-\frac{\left(\varepsilon_i^* - f_i(\alpha)\right)^2}{2 \cdot \sigma^2}\right). \tag{4}$$

Then, the likelihood of each crack length within the finely discretized range is calculated as the product of the likelihoods corresponding to each individual strain gauge direction that is selected and activated in the tested strain gauge combinations [12]:

$$L = \prod_{i=1}^{n} P_i\left(\varepsilon_i^* - f_i(\alpha); \mu = 0; \sigma^2 = \sigma_\varepsilon^2\right). \tag{5}$$

where n is the number of sensors selected to be activated.

For numerical stability, the natural logarithm of likelihood (log-likelihood) is employed, whereby the total log-likelihood is now the sum of the individual terms [10]:

$$logL = \sum_{i=1}^{n} P_i\left(\varepsilon_i^* - f_i(\alpha); \mu = 0; \sigma^2 = \sigma_\varepsilon^2\right). \tag{6}$$

For each set of observations, the crack length that maximizes the total log-likelihood is identified. This value is equivalent to the one that maximizes the Gaussian likelihood function, since the logarithm is a monotonically increasing transformation, and it is identified numerically as [10]:

$$(\hat{a}, \hat{\sigma_E})_{MLE} = arg \max_{a} \log(L(\hat{\alpha}, \hat{\sigma_E}, \{\varepsilon_\kappa^*\})). \quad (7)$$

The value $\hat{a}$ is the MLE-based estimate of the crack length that corresponds to a specified strain vector, maximizing the likelihood that the deviation E_i is close to zero, within the finely discretized crack length range. This procedure is repeated across the target crack length range to statistically assess the accuracy of the Maximum Likelihood Estimation-based damage identification approach over the entire range.

4. Evaluation Results

The assessment process involved evaluating the response of each strain gauge measurement direction individually, as defined and located in Figure 1. This was followed by assessments of combinations of two and three strain components to determine the optimal configuration for accurate crack length estimation under uncertainty while minimizing the number of strain gauges used.

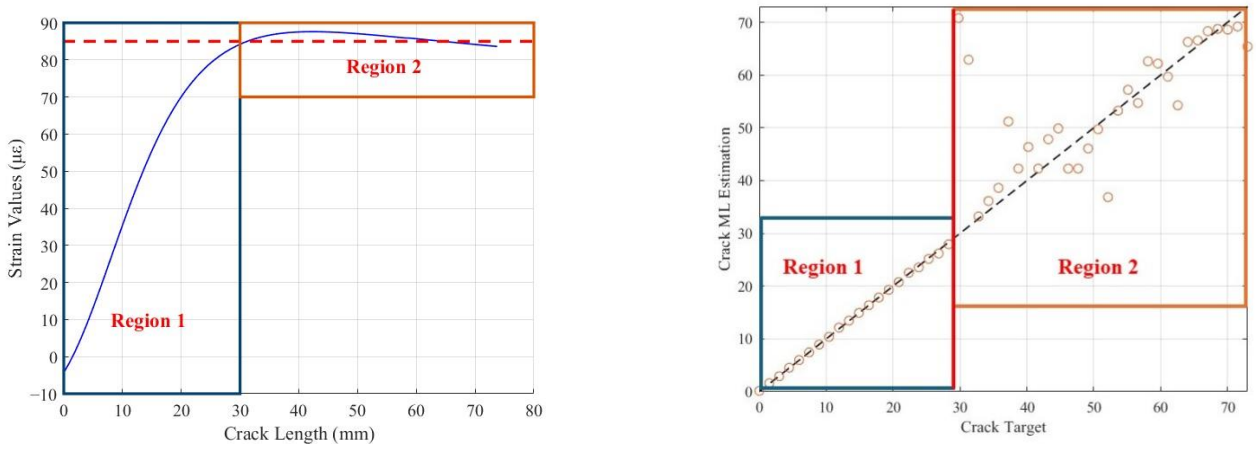
To visualize the results of the maximum likelihood estimates, each estimate is plotted against its corresponding target crack length along with a 45° reference line ($y = x$) to assess agreement. Points that lie on the reference line indicate perfect agreement, while increasing deviation from the line reflects decreasing accuracy.

When using a single strain component measured along a specific direction, both the strain behaviour and the accuracy of the Maximum Likelihood Estimator (MLE) are influenced by the proximity of the crack to each strain gauge. The finite element (FE) model predictions of crack length versus strain behaviour, shown in Figure 2a, indicate that when the crack propagates close to the location of the strain gauge, where it showcases higher sensitivity, the strain values exhibit a monotonic, one-to-one relationship with crack length, as illustrated in region 1 of Figure 2a. However, as the crack propagates further from the strain gauge, within an area it exhibits less sensitivity, the relationship between the strain values and the crack lengths becomes non-monotonic, as demonstrated in region 2 of Figure 2a, with a single strain value corresponding to two distinct crack lengths.

In Figure 2b, the Maximum Likelihood Estimators (MLEs) are plotted against target crack lengths along a 45° reference line. Higher accuracy, indicated by points aligning closely with the reference line, is observed in region 1, as the crack propagates near the strain gauge whose measurements were used to perform the estimation. As the crack propagates further away, accuracy decreases as reflected by points deviating more from the reference line, as seen in region 2.

These results indicate that strain gauges are most effective when the crack propagates near their location, producing a monotonic strain-crack behaviour and reliable maximum likelihood estimates.

To achieve optimal accuracy throughout the entire crack propagation range, it is observed that strain gauges should be selected and combined based on their sensitivity to the different stages of crack growth. With the objective of improving the accuracy of the estimations, combinations of strain components were tested, initially in pairs and subsequently in groups of three.



(**a**) (**b**)

Figure 2. Response of strain gauge 1 in the y-direction (Its specified location and direction is shown in Figure 1): (**a**) FE-model predictions of strain values as a function of crack length, showcasing two regions. Region 1 (0–30 mm) exhibits linear behaviour, while Region 2 (>30 mm) a non-linear one. (**b**) Comparison between the target crack length and the corresponding Maximum Likelihood Estimations (MLE). Region 1 demonstrates high accuracy with estimates closely on the ideal line ($y = x$), while in region 2 increased deviation from the ideal line reflects reduced prediction accuracy. Each circular marker presents an individual data point comparing the maximum likelihood estimate against the target crack length value. The dashed line represents the ideal prediction line ($y = x$), indicating the perfect agreement.

During the evaluation of two-component combinations, it was observed that certain pairs yielded higher estimation accuracy. A representative high-accuracy pair consists of strain gauge 2 measuring strain along the x-direction and strain gauge 3 along the y-direction, as illustrated in Figure 3, providing accurate estimates over the entire crack length range, with data points nearly perfectly aligned with the reference line.

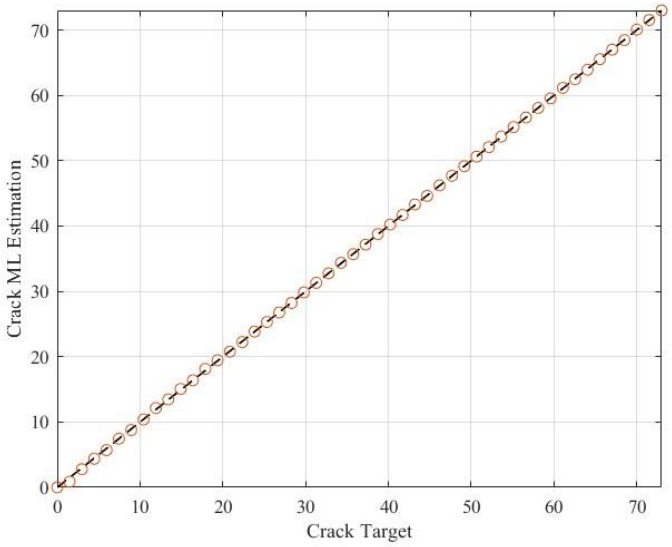


Figure 3. Comparison between the target crack length and the corresponding Maximum Likelihood Estimations (MLE) when strain gauge 2 (direction x) and strain gauge 3 (direction y) are activated (Their locations shown in Figure 1). Each circular marker presents an individual data point comparing the maximum likelihood estimation against the target crack length value. The dashed line represents the ideal prediction line ($y = x$), indicating the perfect agreement.

When evaluating combinations of three different strain components, several configurations achieved very high accuracy. One of them is the configuration involving strain gauge 1 in the y-direction and strain gauge 3 in both directions (Figure 4) which yielded estimations consistently accurate across all crack lengths.

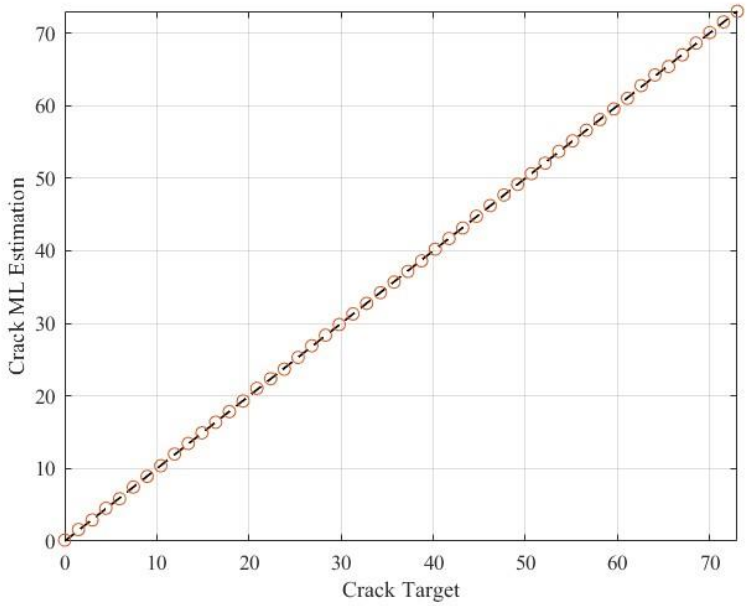


Figure 4. Comparison between the target crack length and the corresponding Maximum Likelihood Estimations (MLE) when strain gauge 1 (direction y) and strain gauge 3 (both directions) are activated (Their locations shown in Figure 1). Each circular marker presents an individual data point comparing the maximum likelihood estimation against the target crack length value. The dashed line represents the ideal prediction line ($y = x$), indicating the perfect agreement.

Based on the results of the various configurations, it is observed that achieving high estimation accuracy requires the inclusion of strain gauges recording strain in both directions and exhibiting sensitivity across different regions of the crack length range.

5. Concluding Remarks

Overall, based on the assessment of the results from various sensor configurations, strain sensing data acquired from strategically placed sensors successfully estimate the crack length under different sources of uncertainty, in a numerical environment. While individual strain components provide accurate estimations within localized regions of crack growth, combining multiple strain components from different locations and directions significantly improves estimation accuracy across the entire crack propagation range. The automation of optimal sensor placement selection, the experimental validation of the proposed approach and the extension to more complex geometries could be included in future research.

Author Contributions: Conceptualization, K.A.; methodology, A.V. and K.A.; software, A.V.; validation, A.V.; formal analysis, A.V.; investigation, A.V.; resources, N.S. and K.A.; data curation, N.S. and K.A.; writing—original draft preparation, A.V.; writing—review and editing, N.S. and K.A.; visualization, A.V.; supervision, N.S. and K.A.; project administration, K.A.; funding acquisition, K.A. All authors have read and agreed to the published version of the manuscript.

Funding: This research received no external funding.

Institutional Review Board Statement: Not applicable.

Informed Consent Statement: Not applicable.

Data Availability Statement: The data presented in this study are available on request from the corresponding author.

Conflicts of Interest: The authors declare no conflicts of interest.

References

1. Vasudevan, A.; Sadananda, K.; Iyyer, N. Fatigue damage analysis: Issues and challenges. *Int. J. Fatigue* **2015**, *82*, 120–133. [CrossRef]
2. Han, T.; Wu, G.; Lu, Y. Crack monitoring using short-gauged Brillouin fiber optic sensor. *Measurement* **2021**, *179*, 109461. [CrossRef]
3. Argyris, C.; Chowdhury, S.; Zabel, V.; Papadimitriou, C. Bayesian optimal sensor placement for crack identification in structures using strain measurements. *Struct. Control Health Monit.* **2018**, *25*, e2137. [CrossRef]
4. Tatsis, K.; Agathos, K.; Chatzi, E.; Dertimanis, V. A hierarchical output-only Bayesian approach for online vibration-based crack detection using parametric reduced-order models. *Mech. Syst. Signal Process.* **2022**, *167*, 108558. [CrossRef]
5. Papadimitriou, C.; Fritzen, C.-P.; Kraemer, P.; Ntotsios, E. Fatigue predictions in entire body of metallic structures from a limited number of vibration sensors using Kalman filtering. *Struct. Control Health Monit.* **2011**, *18*, 554–573. [CrossRef]
6. Yu, L.; Giurgiutiu, V.; Ziehl, P.; Ozevin, D.; Pollock, P. Steel Bridge Fatigue Crack Detection with Piezoelectric Wafer Active Sensors. In Proceedings of the Sensors and Smart Structures Technologies for Civil, Mechanical, and Aerospace Systems, San Diego, CA, USA, 8–11 March, 2010, SPIE-The International Society for Optical Engineering: Bellingham, WA, USA, 2010; Volume 7647. [CrossRef]
7. Knott, J.F. *Fundamentals of Fracture Mechanics*; Butterworths: London, UK, 1973; pp. 106–107.
8. *ASTM A131*; Standard Specification for Structural Steel for Ships. ASTM International: West Conshohocken, PA, USA, 2019.
9. Makris, P.; Silionis, N.E.; Anyfantis, K.N. Spectral fatigue analysis of ship structures based on a stochastic crack growth state model. *Int. J. Fatigue* **2023**, *176*, 107878. [CrossRef]
10. Casella, G.; Berger, R.L. *Statistical Inference*, 2nd ed.; Duxbury: Pacific Grove, CA, USA, 2002; pp. 315–323.
11. Bishop, C.M. *Pattern Recognition and Machine Learning*, 1st ed.; Springer: New York, NY, USA, 2006; pp. 140–143.
12. Walpole, R.E.; Myers, R.H.; Myers, S.L.; Ye, K. *Probability & Statistics for Engineers & Scientists*, 9th ed.; Pearson: London, UK, 2016; pp. 85–89, 327–332.

Disclaimer/Publisher's Note: The statements, opinions and data contained in all publications are solely those of the individual author(s) and contributor(s) and not of MDPI and/or the editor(s). MDPI and/or the editor(s) disclaim responsibility for any injury to people or property resulting from any ideas, methods, instructions or products referred to in the content.